

# Vibrotactile Rendering of Splashing Fluids

Gabriel Cirio, Maud Marchal, Anatole Lécuyer, and Jeremy R. Cooperstock

**Abstract**—We introduce the use of vibrotactile feedback as a rendering modality for solid-fluid interaction, based on the physical processes that generate sound during such interactions. This rendering approach enables the perception of vibrotactile feedback from virtual scenarios that resemble the experience of stepping into a water puddle or plunging a hand into a volume of fluid.

**Index Terms**—vibrotactile rendering, computational fluid dynamics, air bubbles, sound generation

## 1 INTRODUCTION

A major concern of virtual reality (VR) is the simulation of highly realistic virtual environments. Among the possible feedback modalities, haptics plays an important role in the realistic perception of the size, shape and material of objects constituting the surrounding environment. In this context, several researchers have recently demonstrated encouraging results by modeling and rendering different materials through high-frequency vibrations. For example, several solid materials can be perceived through measurement-based approaches [1]–[4], while physically based approaches have been used for simulating both solids such as wood and metal [5] and aggregates such as gravel and snow [6]. Display can be achieved by the wide availability of off-the-shelf and easily built vibrotactile hardware (actuated floors [7], shoes [8], and hand-held transducers [9]) supporting bodily interaction with virtual materials. The addition of such vibrotactile rendering to the complementary visual and acoustic modalities can enhance the quality of the display, as suggested by recent perceptual studies [11], increasing the degree of realism, and in turn, improve user immersion. In this manner, compelling virtual reality (VR) scenarios involving physically based virtual materials have been demonstrated using hand-based and foot-based interaction with visual and vibrotactile feedback [6], [10].

However, some materials, such as water and other fluids, have been largely ignored in this context. For VR simulations of real-world environments, the inability to include interaction with fluids is a significant limitation. Potential applications include improved training involving fluids, such as medical and phobia simulators, and enhanced user experience in entertainment, such as when interacting with water in immersive virtual worlds. The work described here represents an initial

effort to remedy this limitation, motivated by our interest in supporting multimodal VR simulations such as walking through puddles or splashing on the beach.

To this end, the main contribution of this paper is the introduction of the first physically based vibrotactile fluid rendering model for solid-fluid interaction. Such an approach offers the benefits not only of generating a potentially realistic response but of doing so in a manner that is automatically synchronized across modalities, and that scales automatically in terms of fluid behavior and the corresponding intensity of the perceived feedback. The beach and the bucket scenarios, in the video accompanying this paper, illustrate the advantages of using a physically based approach.

Similar to other rendering approaches for virtual materials [5], [6], [10], we leverage the fact that vibrotactile and acoustic phenomena share a common physical source. Hence, we base the design of our vibrotactile model on prior knowledge of fluid sound rendering, as vibrational effects are very likely induced by the same phenomenon in nature. Since fluid sound is generated mainly through bubble and air cavity resonance, we enhanced our fluid simulator with real-time bubble creation and solid-fluid impact mechanisms. The corresponding interaction and simulation events are fed to our novel vibrotactile rendering component, which follows different signal generation mechanisms to produce a perceptually compelling feedback. Using this approach, we are investigating the use of bubble-based vibrations to convey splashing fluid interaction sensations to users without requiring additional kinesthetic cues. We render the feedback for hand-based and, in a more innovative way, for foot-based interaction, engendering a rich perceptual experience of feeling the sensations of water.

## 2 RELATED WORK

Recent work has focused on the vibrotactile feedback of virtual materials. Through a measurement-based approach, Okamura et al. [1], [2] used real contact information with a decaying sinusoidal signal to provide perceptual vibrotactile information about the stiffness of rigid

- 
- G. Cirio, M. Marchal, and A. Lécuyer are with INRIA Rennes, France. E-mail: {gcirio, mmarchal, alecuyer}@inria.fr
  - M. Marchal is also with INSA Rennes, France
  - J. R. Cooperstock is with the Centre for Intelligent Machines, McGill University. E-mail: jer@cim.mcgill.ca

materials such as rubber, wood and aluminium. Kuchenbecker et al. [3] improved this approach by adapting the signal to the dynamic response of the device using an inverted system model of the display. Romano and Kuchenbecker [4] synthesized a wider range of solid materials by reconstructing a signal from recorded samples stored as frequency-domain models for an efficient signal prediction based on speed and force inputs. All physically based approaches, however, rely on the principle of using a common model to generate acoustic and vibrotactile feedback, due to the common physical source of both phenomena in an interaction context. Visell et al. [6] use an aggregate model to simulate snow, gravel and sand, which is rendered through tiles equipped with vibrotactile transducers. Using the same devices, a fracture model is used to simulate the cracking ice of a frozen pond [10]. Papetti et al. [8] use various acoustic models from the Sound Design Toolkit [12] to generate the vibrations of crumpling materials. The signals are displayed through custom shoes equipped with loudspeakers and haptic actuators. Nordahl et al. [5] developed a similar approach with rigid, friction and aggregate models. They conducted a material recognition experiment, showing that some material properties could be conveyed through haptic rendering alone.

Following these aforementioned approaches for ground material rendering, we aim at leveraging real-time fluid sound synthesis algorithms to generate the relevant vibrotactile feedback. Those techniques that are physically based rely on the oscillation of air bubbles trapped inside the fluid volume [13] to produce sound. The first bubble sound synthesis technique was proposed in Van den Doel’s seminal work [14] where, based on Minnaert formula [15], he provides a simple algorithm to synthesize bubble sounds based on a few parameters. However, the synthesis was not coupled to a fluid simulation. This coupling is achieved by Drioli et al. [16] through an ad-hoc model for the filling of a glass of water, based on the height of the fluid inside the glass and on collision events. Moss et al. [17] propose a simplified, physically inspired model for bubble creation, designed specifically for real-time applications. It uses the fluid surface curvature and velocity as parameters for bubble creation and a stochastic model for bubble sound synthesis based on Van den Doel’s work [14]. However, the model is designed for a shallow water simulator, which greatly reduces interaction possibilities by allowing only surface waves, precluding splashes and object penetration.

Inspired by the physically based fluid sound synthesis work of Moss et al. [17], and utilizing a particle-based fluid model [18], we develop an efficient bubble generation technique (Section 4) and introduce a novel vibrotactile model (Section 5).

### 3 OVERVIEW OF THE APPROACH

Human sensitivity to vibrotactile stimuli ranges approximately from approximately 10 to 1000 Hz, with

Meissner’s (tactile) corpuscles being dominant at lower frequencies, most sensitive around 50 Hz, and the much larger FA II (Pacinian) receptors sensitive to frequencies between 40 and 1000 Hz, optimally sensitive around 250 Hz [19], [20], whereas the human audible range of frequencies extends from 20 Hz to 20 kHz.

When an object vibrates, vibrations travel through the surrounding medium (solid, liquid or gas) to reach the subject’s ears and tactile mechanoreceptors. We motivate our vibrotactile approach, based on sound generation mechanisms, on the fact that both acoustic and tactile feedback vibrations share a common physical source.

By comparing film frames with the air-borne generated sound, Richardson [13] provides an explanation for the process of a projectile impacting and entering a fluid volume. The impact produces a “slap” and projects droplets, while the object penetration creates a cavity that is filled with air. The cavity is then sealed at the surface, creating an air bubble that vibrates due to pressure changes. Smaller bubbles can spawn from the fragmentation of the main cavity, as well as from the movement of the fluid-air interface, such as when the droplets return to the fluid volume.

Our vibrotactile model is therefore divided in three components, following the physical processes that generate sound during solid-fluid interaction [13], [21]: (1) the initial high frequency impact, (2) the small bubble harmonics, and (3) the main cavity oscillation. As a consequence, it is highly dependent on the efficient generation and simulation of air bubbles within the fluid. Hence, a real-time fluid simulator enhanced with bubble synthesis is required on the physical simulation side.

Figure 1 provides an overview of our approach. The physical simulator automatically detects the solid-fluid impacts and the creation of air bubbles caused by interaction between a solid (such as a foot, hand, or object) and the fluid volume. For each of these events, it sends the corresponding message to the vibrotactile model, which synthesizes a vibrotactile signal according to the simulation parameters. The signal is then output through a specific vibrotactile device, such as an actuated tile for foot-fluid interaction or a hand-held vibrator for hand-fluid interaction. This enables rich body-fluid interactions with vibrotactile and multi-modal cues (Sections 6 and 7), resulting in positive user feedback (Section 8).

## 4 FLUID SIMULATION WITH BUBBLES

The first building block of our approach is the fluid volume itself: we require a physically based real-time fluid simulation. Among existing fluid simulation techniques, the Smoothed-Particle Hydrodynamics (SPH) [18] model fulfills our requirements well, since the resulting fluid is unbounded, fast to compute and preserves small-scale details such as droplets. The simulated media, in this case fluid, is discretized into a set of particles carrying different physical attributes, such as mass and viscosity. SPH interpolates an attribute  $Q_i$  at any position  $\mathbf{x}$  in

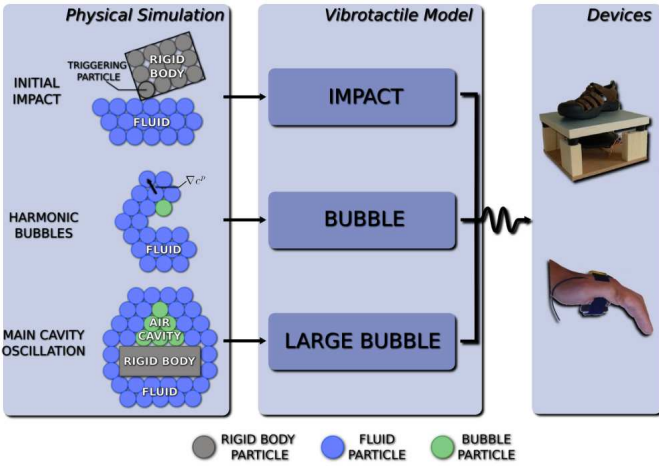


Fig. 1. Overview of our approach: the physical simulation computes the different parameters that are fed to the 3-step vibrotactile model, producing the signal sent to the various vibrotactile displays (Top: actuated tile [7]. Bottom: hand-held vibrator [9]).

space from attributes  $Q_j$  sampled at neighboring particle locations  $\mathbf{x}_j$  as

$$Q_i = \sum_j Q_j V_j W(\mathbf{x} - \mathbf{x}_j, h), \quad (1)$$

where  $V_j$  is the volume of particle  $j$ , and  $W$  is the smoothing kernel of support  $h$ , where particles beyond  $h$  are not taken into account.

The motion of fluids is driven by the Navier-Stokes equations. Using the implementation of these equations in the SPH model [22], pressure and viscosity forces are computed at each time step. Rigid bodies are simulated as a constrained set of particles. For further details, we refer the reader to references [23] and [22].

As previously explained, to achieve vibrotactile interaction with fluids we need to simulate the bubbles inside the fluid. Since we are concerned only with bubble creation events resulting to the synthesis of bubble sounds, a bubble has a very short life span within our model, and it can be seen more as an event than as the actual simulation of a pocket of air, i.e., a bubble “vibrates” only when it spawns. However, even though we are interested in only the creation event and not the bubble itself, we need SPH “bubble” particles and a set of rules to detect the events in a physically based manner and to avoid triggering the same event multiple times. Hence, we adopt an existing SPH bubble synthesis algorithm [24] to obtain an efficient bubble creation and deletion mechanism. Since only bubble creation plays an important role, we simplify the original approach by doing only one-way fluid-bubble coupling and using a new set of bubble deletion rules, reducing the complexity, and in turn, the computation time, of the mechanism. Implementing the original approach would not have a significant impact on the resulting vibrotactile feedback.

A bubble is spawned when a volume of fluid entraps a volume of air. In order to detect this phenomenon within the SPH simulation, we compute an implicit color field  $c^p$  as in the method of Muller et al. [24]. This color field quantifies the presence of matter (fluid, rigid and bubble particles) around any position in space, while its gradient  $\nabla c^p$  estimates in which direction the surrounding matter is mainly located. At each timestep, we compute  $\nabla c^p$  at each fluid particle position with:

$$\nabla c_i^p(\mathbf{x}_i) = \sum_j V_j \nabla W(\mathbf{x}_i - \mathbf{x}_j, h). \quad (2)$$

A fluid particle  $i$  triggers a bubble creation if the following conditions are fulfilled:

- the vertical component of  $\nabla c_i^p$  is positive: the fluid particle has most of its surrounding matter above it, creating a pocket of air under it.
- the magnitude of the velocity of the particle is above a threshold: still or slow moving fluid particles do not generate bubbles.

A bubble is destroyed when it is not entrapped by fluid or held by a rigid body anymore. Since we use bubbles only for triggering events, a bubble is also destroyed if it is alone in the surrounding media. To this end, we compute a new implicit color field,  $c^b$ , which considers only bubble particles, thus quantifying the presence of bubbles around a point in space. A bubble  $i$  is destroyed if one of the following conditions is fulfilled:

- the color field  $c_i^b$  is null: the particle is alone inside the media.
- the vertical component of  $\nabla c_i^p$ , estimating the direction of the surrounding matter, is negative: the bubble particle has most of its surrounding particles under it, and the air cannot be trapped anymore.

## 5 VIBROTACTILE MODEL

Our vibrotactile model receives the events from the physical simulation. It can then synthesise a signal through three different components: the initial high frequency impact, the small bubble harmonics, and the main cavity oscillation, as illustrated in Figure 1.

### 5.1 Initial Impact

During rigid body impacts on a fluid surface, Richardson [13] observed a damped high-frequency and low amplitude sound immediately after the impact, later explained as a guided acoustic shock [25]. To the best of our knowledge, no model provides the equations for air pressure oscillations due to a rigid body impact on a fluid surface. Previous work has been able to model the phenomenon to some extent, only for very simple shapes and specific penetration cases [26]. Nevertheless, the short duration of the impact does not justify a computationally expensive implementation. Hence, similar to previous work [16] [27], we use a resonant filter and follow a physically inspired approach exploiting the short and burst-like nature of the vibration.

### 5.1.1 Synthesis

The impact signal is synthesized in a three step approach. A burst of white noise is first generated, spanning the vibrotactile frequency range with a given base amplitude  $A$ . The signal is then fed to a simple envelope generator to modulate its amplitude. The signal rises exponentially during an attack time  $t_a$ , from nil to the original amplitude  $A$ , followed by an exponential decay of release time  $t_r$ , mimicking the creation and attenuation of the short and highly damped impact. Last, the modulated signal excites an elementary resonator. A second-order resonant filter is used, creating a resonance peak around a central frequency  $w_0$ . The impact signal is therefore approximated as a resonating burst of white noise, with parameters to control its amplitude ( $A$ ), duration ( $t_a, t_r$ ) and central frequency ( $w_0$ ).

### 5.1.2 Control

An impact event is triggered when the distance between a rigid body particle and a fluid particle is below the smoothing radius. Since only the particles at the surface of the rigid body have to be taken into account to avoid false triggers, a new implicit color field  $c^r$  is computed considering only rigid body particles: particles belonging to the lowest level sets of  $c^r$  belong to the surface. Richardson [13] observed that, in general, the intensity of the impact sound between a rigid body and a fluid is proportional to  $v^3$ , where  $v$  is the speed of the body at the moment of impact. Hence, after detecting an impact, we can synthesize an impact signal of amplitude  $A$  proportional to  $v^3$ . Perceptually convincing duration and central frequency values were obtained through preliminary testing of a wide range of values. Once set, they remain unchanged for all impacts.

## 5.2 Harmonic Bubbles

Small bubbles are generated by small pockets of air trapped under the water surface. Splashes and underwater cavity fragmentation are two causes for small bubble generation. By approximating all bubbles as spherical bubbles and relying on our SPH simulation enhanced with bubble generation, we can easily synthesize and control this component of the model.

### 5.2.1 Synthesis

Following the physically based approach of van den Doel [14] and modeling the spherical bubble as a damped harmonic oscillator, the pressure wave  $p(t)$  of an oscillating spherical bubble is given by

$$p(t) = A_0 \sin(2\pi t f(t)) e^{-dt}, \quad (3)$$

$A_0$  being the initial amplitude (in meters),  $f(t)$  the resonance frequency (in hertz) and  $d$  a damping factor (in  $s^{-1}$ ).

Minnaert's formula [15] approximates the resonance frequency  $f_0$  (in hertz) of a spherical bubble in an infinite volume of water by  $f_0 \cdot r \approx 3 \text{ Hz}\cdot\text{m}$ , where  $r$  is the

bubble radius (in meters). In order to account for the rising in pitch due to the rising of the bubble towards the surface, Van den Doel [14] introduces a time dependent component in the expression of the resonant frequency:  $f(t) = f_0 \cdot (1 + \xi \cdot d \cdot t)$ , with the dimensionless constant  $\xi = 0.1$  found experimentally. Taking into account viscous, radiative and thermal damping, the damping factor  $d$  is set to  $d = 0.13 \text{ m}\cdot\text{s}^{-1}/r + 0.0072 \text{ m}^{3/2}\cdot\text{s}^{-1}r^{-3/2}$ . As for the initial amplitude  $A_0$ , previous work [28] suggests, after empirical observations, that  $A_0 = \epsilon r$  with  $\epsilon \in [0.01; 0.1]$  as a tunable initial excitation parameter. For a detailed explanation of the different hypotheses and equations, we refer the reader to [17] and [14].

### 5.2.2 Control

Our bubble vibration synthesis algorithm allows the generation of bubble sounds based on two input parameters: the bubble radius  $r$  and the initial excitation parameter  $\epsilon$ . Using our SPH simulation, we couple the vibration synthesis with bubble creation events and automatically select the aforementioned parameters. To simulate the fluid and the bubbles at a scale where the particle radius matches the smallest bubble radius that generates a perceivable vibration (3 mm for a frequency of 1 kHz), we would require approximately four million particles for a cubic meter of fluid. In this case, the computation time would be one order of magnitude greater than current state-of-the-art GPU simulations [23]. Since we cannot directly link the particle radius to the resonating bubble radius, we adopt the physically inspired approach of Moss et al. [17] to determine the parameters: power laws are used for the distributions of both  $r$  and  $\epsilon$ , for which details are provided in the reference [17]. When a bubble is created, these values are computed and sent to the signal synthesis algorithm.

## 5.3 Main Cavity Oscillation

The main cavity is a single bubble with large radius that produces a characteristic low-frequency bubble-like sound. We can thus rely on our harmonic bubble synthesis and control algorithms for this third component of our vibrotactile model.

### 5.3.1 Synthesis

As for the harmonic bubble component (Section 5.2.1), we use Equation 3 to synthesize the vibration produced by the oscillation of the main cavity. Since we will be using larger values for  $r$ , the resulting vibration will be of a much lower frequency, coherent with what we hear in real life.  $\epsilon$  is set to 0.1 since no variability is desired.

### 5.3.2 Control

In order to detect the formation and collapsing of the main cavity during object penetration, we track the grouping of individual bubbles within our SPH simulation. Bubbles are spawned and stay alive when a cavity begins its closing and collapsing process, until

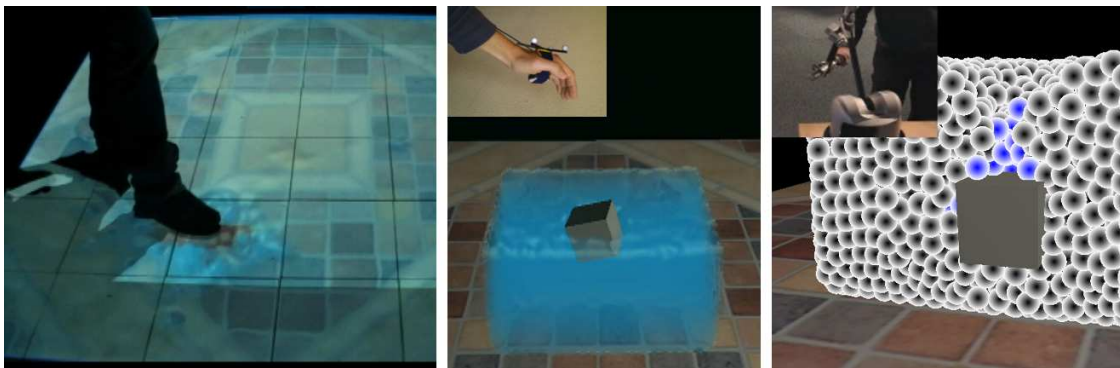


Fig. 2. Interaction examples using different body parts and rendering devices: a foot-water pool scenario using actuated tiles (left), and a hand-water basin scenario using a small vibrator (center) or a 6DoF haptic device (right).

they fill most of the cavity volume, as illustrated in Figure 1 and rendered in Figure 2 (right, bubbles in blue). At this point, there are bubbles within the cavity that are surrounded exclusively by other bubbles. These bubbles are detected when their color field  $c^b$  is above a threshold. If such a particle is detected, there is a potential cavity collapse.

Starting from the detected particle, we perform a search for neighboring bubbles to find the extent of the cavity. Bubble neighbors are added to the set of cavity bubbles, and the process is repeated on the new neighbors until no new neighbor is added. As the search is executed on the GPU, an iterative implementation is required, with one thread per new bubble neighbor. The search is therefore accelerated on the GPU, leveraging the existing neighbor search algorithms and structures of our SPH framework [23], which efficiently find the neighbors of each particle using the GPU. During our experiments, we required less than five search cycles to account for all the bubbles inside a cavity.

The total number  $N_b$  of cavity bubbles is proportional to the volume of the cavity. Since the cavity is modeled as a single large spherical bubble in the signal synthesis algorithm, its radius  $r$  can be deduced from the volume of the cavity. Hence, the number of cavity bubbles is mapped to the radius  $r$  of the spherical cavity, with user-defined minimal ( $r^{min}$ ) and maximal ( $r^{max}$ ) values:  $[N_b^{min}, N_b^{max}] \rightarrow [r^{min}, r^{max}]$ .

## 6 VIBROTACTILE RENDERING

The vibrotactile model is implemented in PureData, while the SPH fluid and bubble simulation are implemented on GPU [23]. The communication between the SPH simulation and the acoustic model is handled through the Open Sound Control (OSC) protocol. Each time a bubble, cavity or impact event is detected in the fluid simulation, an OSC message is sent to the acoustic model with the corresponding parameters for sound synthesis. The following constant values were used for the synthesis of the initial impacts:  $t_a = 0.001$  s,  $t_r = 0.37$  s and  $w_0 = 420$  Hz.

We designed three scenarios representing three possible interaction conditions. For the graphic rendering, we used a meshless screen-based technique optimized for high frequency rendering, described in previous work [23]. The scenarios were run on a Core 2 Extreme X7900 processor at 2.8 GHz, with 4 GB of RAM and an Nvidia Quadro FX 3600M GPU with 512 MB of memory. PureData synthesizes the output signal at a 44 kHz rate, while the simulation frequency depends mainly on the number of particles being simulated, as specified for the different scenarios. The graphic rendering runs in a different GPU. Some of these scenarios can be seen in the video accompanying this paper.

**Active foot-water interaction (shallow pool).** Our approach is particularly suited for foot-floor interaction, where the floor renders the vibrotactile feedback to the user's feet through appropriate vibrotactile transducers. We used a floor consisting of a square array of thirty-six  $30.5 \times 30.5$  cm rigid vibrating tiles [7], rendering in the 20–750 Hz range. The virtual scene consisted of a virtual pool with a water depth of 20 cm filling the floor. The user's feet were modeled as parallelepiped rigid bodies and tracked through the floor pressure sensors. The user could walk about, splashing water as he stepped on the pool as seen in Figure 2 (left). Performance: 15,000 particles (1% bubbles), simulation update rate of 152 Hz.

**Passive foot-water interaction (beach shore).** Using the same hardware setup as the previous scenario, we designed a tidal action scene in which the user stands still and experiences waves washing up on a sandy beach. Performance: 15,000 particles (6% bubbles), simulation update rate of 147 Hz.

**Active hand-water interaction (water basin).** The user can interact with fluids with his hands using a hand-held vibrotactile transducer [9]. In this scenario, a small vibrator was attached to one of the user's hands. The hand was tracked by a motion capture system and modeled in the virtual world as a parallelepiped rigid body. He could feel the water sensations by plunging his hand into a cubic volume of fluid, as seen in Figure 2 (center). Figure 3 shows the vibrotactile signal generated during a plunging movement. Performance: 7,000 particles (6%

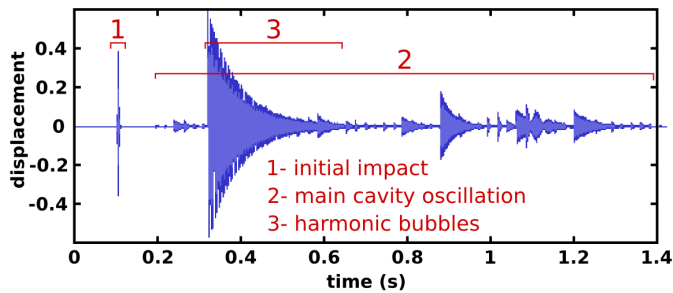


Fig. 3. Vibrotactile signal generated with our model during a plunging movement, with its three distinct components: (1) the initial impact, (2) the small bubble harmonics, and (3) the main cavity oscillation.

bubbles), simulation update rate of 240 Hz.

## 7 EXTENSION TO OTHER MODALITIES

The model can be combined with existing kinesthetic and auditory feedback techniques to achieve a truly multimodal interaction with fluids, as illustrated in the video accompanying this paper.

Kinesthetic feedback from fluids arising from pressure and viscosity forces can be computed through the Navier-Stokes equations and rendered through a suitable haptic device, such as a multiple degrees-of-freedom force-feedback manipulator. The approach using the same SPH fluid and rigid body simulation model [23] is illustrated in Figure 2 (right), which shows a pool of fluid with a rigid body coupled to a Virtuouse 6DoF force-feedback device from Haption.

Since our vibrotactile model is built from sound generation mechanisms, we are able to produce acoustic feedback using the same model, by displaying the signal through a speaker and in the 12 Hz–20 kHz range. Since the sound synthesis is coupled to a physically based fluid simulator, it enables richer interactions than previous real-time ones, where ad-hoc models (for the filling of a glass) [16] or shallow-water equations [17] were used.

## 8 USER FEEDBACK

The novelty of the interaction scenarios, for example, users walking on a volume of fluid and experiencing vibrotactile stimuli, motivated us to design the scenario of a pilot study to assess the perceived interaction qualitatively. The objective of the pilot study was to answer the following questions:

- 1) Can users recognize that they are stepping onto a simulation of water, despite the contradictory perceptual cues provided by the rigid floor surface?
- 2) Does the addition of vibrotactile or acoustic rendering improve the realism of the interaction compared to visual feedback alone?
- 3) How compelling is the overall experience?

## 8.1 Scenario and Results

The scenario required subjects to walk on the *virtual* shallow pool of fluid described in Section 6 and perform both a material identification and a subjective evaluation. On the initial presentation, only vibrotactile feedback was provided, with no graphics or audio. Subjects were instructed to walk freely and were observed to explore most of the surface. They were then asked to identify the simulated material on which they were stepping. The question was open: no material suggestions were given, and particular attention was paid to avoid providing any verbal cues to the participants. Since the equipment used generates auditory output in conjunction with vibrotactile feedback, we masked the audio by supplying sufficiently loud pink noise through four speakers surrounding the floor and headphones worn by the users. The users were then presented three different feedback conditions: visual feedback alone (V), visual + audio feedback (V+A) and visual + vibrotactile feedback (V+Vi), counterbalanced across participants and with three repetitions (nine trials per participant). The V+A+Vi condition could not be tested due to the strong residual sound emitted by the tiles when rendering the vibrotactile signal, and to the limited audio bandwidth of the tiles. For each of the three feedback conditions, the users were asked to walk on the actuated floor for 20 seconds and complete a questionnaire, rating each condition on a seven-point Likert scale in terms of *believability* and *engagement* of the interaction.

Feedback was gathered from eight users, all naïve to the purpose of the simulation. We applied a Friedman test statistical analysis to the different conditions, with boxplots of the results shown in Figure 4. The post-hoc analysis was performed using Wilcoxon tests. The reported p-values are adjusted for multiple comparisons and are statistically different at the 5% level ( $p = 0.05$ ). The Friedman test on the *believability* question did not reveal any significant effect of condition ( $\chi^2 = 2.27$ , p-value= 0.06). The Friedman test on the *engagement* question revealed a significant effect of condition ( $\chi^2 = 2.40$ , p-value= 0.04). The post-hoc analysis indicated that the V+Vi condition received significantly higher scores (p-value= 0.04,  $r=0.3311075$ ) than the V condition.

## 8.2 Discussion

The responses to our material identification question, with the presentation of only vibrotactile feedback, were highly encouraging. Six out of the eight subjects stated that they were interacting directly or indirectly with water. This user feedback suggests that our vibrotactile model, based on bubble vibrations, can efficiently convey the sensation of interacting with a fluid volume.

Further insights are available from these responses. Of the six correct answers, two directly identified water, and the remaining four answered that they were walking on “plastic bottles with water inside”, “a floor with wet shoes”, “a water bed”, and “a plank on top of water”. In

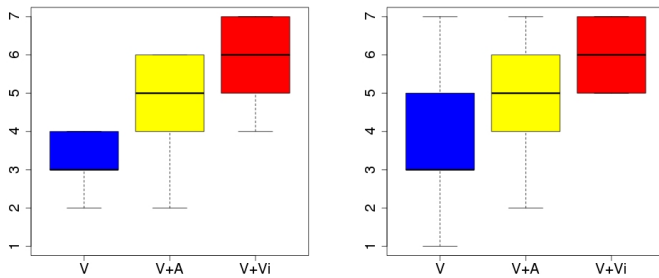


Fig. 4. Boxplots comparing the grades of the three conditions for *believability* and *engagement* criteria. Each boxplot is delimited by the 25% and 75% quartiles of the distribution of the effect over the individuals. The median is also represented for each effect.

other words, most of the subjects who associated their experience with water felt that they were interacting with water through a solid material. We believe the lack of kinesthetic feedback of a sinking foot induced the perception of an intermediate rigid material between the foot and the water. These rigid cues might also have been the reason for the incorrect answers from the two remaining subjects, who replied “wood” and “metal”. We suggest two possible mechanisms for overcoming this sensory conflict: one involving shoes with vibrating soles to provide the vibrotactile rendering, so that stimuli can be presented prior to contact with the real floor; and a second, employing a vibromechanical actuator, as used in earlier prototypes [7], to deliver the necessary kinesthetic cues associated with foot-fluid interaction.

As expected, the subjective feedback provided by the users confirmed that the use of vibrotactile feedback improved the interaction experience compared to having only visual rendering. More importantly, the results also suggest that the addition of vibrotactile feedback is more valuable for solid-fluid interaction than visual rendering alone in terms of the engagement of the experience; it also improved believability, although based on our limited subject pool, the result was not significant. These results show that, despite the lack of kinesthetic feedback to compensate for the conflicting sensory cues provided by the contact of the foot with a rigid tiled floor surface, the effect was perceptually compelling.

## 9 CONCLUSION

In this paper, we introduced the use of vibrotactile feedback as a rendering modality for solid-fluid interaction. We proposed a novel vibrotactile model based on prior fluid sound rendering knowledge, leveraging the fact that acoustic and vibrotactile phenomena share a common physical source. The model is divided into three components: an initial impact with the fluid surface, a cavity oscillation created when the body enters the fluid, and a set of small bubble harmonics. We illustrated this approach with several fluid interaction scenarios, where users felt the fluid through vibrotactile transducers. User

feedback regarding material identification solely based on vibrotactile cues suggested that the model effectively conveys the sensation of interacting with fluids, while highlighting the need for consistent kinesthetic cues.

Future work will focus on using our model with other vibrotactile devices, such as actuated shoes and gloves, as well as providing a more distributed rendering of the signals by leveraging this new hardware. We would also like to evaluate the user perception of their interaction with fluid in different application scenarios.

## REFERENCES

- [1] A. M. Okamura, J. T. Dennerlein, and R. D. Howe, “Vibration feedback models for virtual environments,” in *IEEE International Conference on Robotics and Automation*, pp. 674–679, 1998.
- [2] A. M. Okamura, M. R. Cutkosky, and J. T. Dennerlein, “Reality-based models for vibration feedback in virtual environments,” *IEEE/ASME Transactions on Mechatronics*, vol. 6, no. 3, pp. 245–252, 2001.
- [3] K. J. Kuchenbecker, J. Fiene, and G. Niemeyer, “Improving contact realism through event-based haptic feedback,” *IEEE Transactions on Visualization and Computer Graphics*, vol. 12, no. 2, pp. 219–230, 2006.
- [4] J. Romano and K. Kuchenbecker, “Creating realistic virtual textures from contact acceleration data,” *IEEE Transactions on Haptics*, to appear.
- [5] R. Nordahl, A. Berrezag, S. Dimitrov, L. Turchet, V. Hayward, and S. Serafin, “Preliminary Experiment Combining Virtual Reality Haptic Shoes and Audio Synthesis,” in *Haptics: Generating and Perceiving Tangible Sensations*, 2010, pp. 123–129.
- [6] Y. Visell, J. Cooperstock, B. Giordano, K. Franinovic, A. Law, S. McAdams, K. Jathal, and F. Fontana, “A vibrotactile device for display of virtual ground materials in walking,” in *Haptics: Perception, Devices and Scenarios*, pp. 420–426, 2008.
- [7] Y. Visell, J. Cooperstock, and K. Franinovic, “The EcoTile: an architectural platform for Audio-Haptic simulation in walking,” in *Enactive Interfaces Proc.*, 2007.
- [8] S. Papetti, F. Fontana, M. Civolani, A. Berrezag, and V. Hayward, “Audio-tactile Display of Ground Properties Using Interactive Shoes,” in *Haptic and Audio Interaction Design*, pp. 117–128, 2010.
- [9] H. Yao and V. Hayward, “Design and analysis of a recoil-type vibrotactile transducer,” *The Journal of the Acoustical Society of America*, vol. 128, no. 2, p. 619, 2010.
- [10] Y. Visell, A. Law, J. Ip, S. Smith, and J. Cooperstock, “Interaction capture in immersive virtual environments via an intelligent floor surface,” in *IEEE Virtual Reality Proc.*, pp. 313–314, 2010.
- [11] Pedrosa, R. and MacLean, K. E., “Perception of Sound Renderings via Vibrotactile Feedback.” of IEEE WorldHaptics ‘11, Istanbul, Turkey, pp. 361–366, June 2011.
- [12] M. Rath, F. Avanzini, N. Bernardini, G. Borin, F. Fontana, L. Ottaviani, and D. Rocchesso, “An introductory catalog of computer-synthesized contact sounds, in real-time,” in *Colloquium on Musical Informatics Proc.*, pp. 103–108, 2003.
- [13] E. G. Richardson, “The sounds of impact of a solid on a liquid surface,” *Proceedings of the Physical Society. Section B*, vol. 68, no. 8, pp. 541–547, 1955.
- [14] K. v. d. Doel, “Physically based models for liquid sounds,” *ACM Trans. Appl. Percept.*, vol. 2, no. 4, pp. 534–546, 2005.
- [15] M. Minnaert, “On musical air-bubbles and the sounds of running water,” *Philosophical Magazine Series 7*, vol. 16, no. 104, pp. 235 – 248, 1933.
- [16] C. Drioli and D. Rocchesso, “Acoustic rendering of particle-based simulation of liquids in motion,” *Journal on Multimodal User Interfaces*, pp. 1–9, 2011.
- [17] W. Moss, H. Yeh, J. Hong, M. C. Lin, and D. Manocha, “Sounding liquids: Automatic sound synthesis from fluid simulation,” *ACM Trans. Graph.*, vol. 29, no. 3, pp. 1–13, 2010.
- [18] J. J. Monaghan, “Smoothed particle hydrodynamics,” *Annual Review of Astronomy and Astrophysics*, vol. 30, no. 1, pp. 543–574, 1992.

- [19] M. F. Bear, B. W. Connors, and M. A. Paradiso, "Neuroscience: Exploring the Brain", Lippincott Williams & Wilkins; Third edition, 2006.
- [20] M. Hollins, S. Bensmaïa, and E. Roy, "Vibrotacton and texture perception," *Behavioural Brain Research*, vol. 135, no. 2, pp. 51–56, 2002.
- [21] G. J. Franz, "Splashes as sources of sound in liquids," *The Journal of the Acoustical Society of America*, vol. 31, no. 8, pp. 1080–1096, 1959.
- [22] M. Muller, D. Charypar, and M. Gross, "Particle-based fluid simulation for interactive applications," in *ACM SIGGRAPH/Eurographics Symp. on Comp. Animation Proc.*, pp. 154–159, 2003.
- [23] G. Cirio, M. Marchal, S. Hillaire, and A. Lecuyer, "Six Degrees-of-Freedom haptic interaction with fluids," *IEEE Transactions on Visualization and Computer Graphics*, vol. 17, no. 11, pp. 1714–1727, 2011.
- [24] M. Muller, B. Solenthaler, R. Keiser, and M. Gross, "Particle-based fluid-fluid interaction," in *ACM SIGGRAPH/Eurographics Symp. on Comp. Animation Proc.*, pp. 237–244, 2005.
- [25] M. Lesser, "Thirty years of liquid impact research: a tutorial review," *Wear*, vol. 186-187, Part 1, pp. 28–34, 1995.
- [26] S. Howison, J. Ockendon, and J. Oliver, "Deep- and shallow-water slamming at small and zero deadrise angles," *Journal of Engineering Mathematics*, vol. 42, no. 3, pp. 373–388, 2002.
- [27] V. L. Guruswamy, J. Lang, and W. Lee, "IIR filter models of haptic vibration textures," *IEEE Transactions on Instrumentation and Measurement*, vol. 60, no. 1, pp. 93–103, 2011.
- [28] M. S. Longuet-Higgins, "An analytic model of sound production by raindrops," *Journal of Fluid Mechanics*, vol. 214, pp. 395–410, 1990.